A sex-ratio Meiotic Drive System in Drosophila simulans. II: An X-linked Distorter

A *sex-ratio* Meiotic Drive System in *Drosophila simulans*. II: An X-linked Distorter

Yun Tao[1,2*], Luciana Araripe[1], Sarah B. Kingan[1], Yeyan Ke[1], Hailian Xiao[2], Daniel L. Hartl[1]

1 Department of Organismic and Evolutionary Biology, Harvard University, Cambridge, Massachusetts, United States of America, **2** Department of Biology, Emory University, Atlanta, Georgia, United States of America

The evolution of heteromorphic sex chromosomes creates a genetic condition favoring the invasion of *sex-ratio* meiotic drive elements, resulting in the biased transmission of one sex chromosome over the other, in violation of Mendel's first law. The molecular mechanisms of *sex-ratio* meiotic drive may therefore help us to understand the evolutionary forces shaping the meiotic behavior of the sex chromosomes. Here we characterize a *sex-ratio* distorter on the X chromosome (*Dox*) in *Drosophila simulans* by genetic and molecular means. Intriguingly, *Dox* has very limited coding capacity. It evolved from another X-linked gene, which also evolved de nova. Through retrotransposition, *Dox* also gave rise to an autosomal suppressor, *not much yang* (*Nmy*). An RNA interference mechanism seems to be involved in the suppression of the *Dox* distorter by the *Nmy* suppressor. Double mutant males of the genotype *dox; nmy* are normal for both *sex-ratio* and spermatogenesis. We postulate that recurrent bouts of *sex-ratio* meiotic drive and its subsequent suppression might underlie several common features observed in the heterogametic sex, including meiotic sex chromosome inactivation and achiasmy.

Citation: Tao Y, Araripe L, Kingan SB, Ke Y, Xiao H, et al. (2007) A *sex-ratio* meiotic drive system in *Drosophila simulans*. II: An X-linked distorter. PLoS Biol 5(11): e293. doi:10.1371/journal.pbio.0050293

Introduction

Sex chromosomes are believed to evolve from a pair of autosomes [1–3]. An incipient Y chromosome, like an autosome, is largely euchromatic and free to recombine, except for a small region determining sex, as exemplified by species such as the papaya plant [4] and the medaka and stickleback fish [5,6]. On an evolutionary time scale, the nonrecombining region of the Y will generally expand to include most or all of the chromosome, accompanied by an accumulation of transposable elements and other repetitive sequence, as well as mutational inactivation of most of the protein-coding genes. Only a small number of genes remain active in a mature Y chromosome, such as that in humans or *Drosophila*. Some Y-linked genes are vestiges of the degeneration process, while others have originated from autosomes as a result of recruiting male-specific genes such as those that function in spermatogenesis [7–10]. Accompanying the evolution of sex chromosomes, at least two problems of biological significance arise. One problem is the unequal gene dosage of sex-linked genes between the XY sex and the XX sex. Because of Y degeneration, most genes on the X have only one active copy in the XY sex but two in the XX sex. Myriad strategies to compensate the dosage inequality have been exploited by various species, and some of these mechanisms are now understood in molecular detail in model organisms of fly, worm, and mouse [11].

Another substantial but less obvious problem consists of genetic conflicts over the sex ratio among various parts of a genome, which would allow optimal transmission of their own genes. A corollary to sexual reproduction is Fisher's well-known principle that the sex ratio must be equal for a panmictic population of dioecious species [12]. However, as noted long ago, Fisher's principle applies only to autosomal genes but not to sex-linked genes. Genes linked to one or the other sex chromosome would have a selective advantage were the sex ratio in the population skewed [13]. Because of the genetic isolation between the sex chromosomes, mutations biasing the sex ratio can easily accumulate and enhance each other as long as their deleterious effects are offset by their biased transmission. Thus, the evolution of sex chromosomes leads to an intrinsic conflict among the X, the Y, and the autosomes with regard to sex ratio.

Many cases of sex ratio distortion (*sex-ratio* hereafter) have been documented, particularly in taxa where intensive laboratory investigation is possible [14]. Because of the biased sex ratio, suppressors unlinked to a distorter are strongly selected to restore the Fisherian sex ratio [15]. The occurrence of *sex-ratio* in a population can often be transient and easily escape notice. However, recurrent bouts of *sex-ratio* invasion and suppression can modify the genetic architecture of gametogenesis to such an extent that hybrid incompatibility can be driven to evolve among isolated populations. In other words, genetic conflicts can be a key mechanism for speciation [16–18].

Several cases of *sex-ratio* have been reported in *D. simulans* [19–23]. In a companion paper, we reported the cloning of an autosomal *sex-ratio* suppressor [24]. As Fisher's principle

Academic Editor: Daniel Barbash, Cornell University, United States of America

Received April 12, 2007; **Accepted** September 17, 2007; **Published** November 6, 2007

Abbreviations: aa, amino acids; DAPI, 4′,6-diamidino-2-phenylindole; dsRNA, double-stranded RNA; IR, inverted repeats; MSCI, meiotic sex chromosome silencing; MSUD, meiotic silencing of unpaired DNA; ORF, open reading frame; RACE, rapid amplification of cDNA ends; RT-PCR, reverse-transcription PCR; siRNA, small interfering RNA; TEM, transmission electron microscopy; TGS, transcriptional gene silencing

* To whom correspondence should be addressed. E-mail: ytao3@emory.edu

Author Summary

Mendel's first law of genetics states that two alleles of a heterozygote are transmitted to the next generation at an equal ratio. The cornerstone of population genetics, this law states that the evolutionary fate of genetic variants is solely governed by their contribution to the good of their carriers. However, meiotic drive genes—which skew transmission in their own favor—can evolve under certain circumstances, even though they cause harm to the genome as a whole. Meiotic drive elements are often enriched on the two sex chromosomes (i.e., the X and the Y) because of a lack of recombination between them. Here we describe the genetic and molecular characterization of a meiotic drive distorter on the X chromosome in *Drosophila simulans*. This distorter apparently formed de nova from yet another new gene. To fight back against this harmful distorter, the *D. simulans* genome has evolved an ingenious mechanism based on DNA sequence homology. We postulate that repeated meiotic drive invasion and its suppression could be a major mechanism for genome evolution, underlying the ultimate cause for the inactivation of sex chromosome during meiosis and the occasional loss of recombination (achiasmy), which is observed only in the heterogametic (XY) sex.

predicts, there must exist an X-linked *sex-ratio* distorter to which this suppressor corresponds. Here we report the characterization of such a distorter. More generally, we speculate that *sex-ratio* distortion might underlie the evolution of meiotic sex chromosome inactivation and achiasmatic meiosis, two biological phenomena whose evolutionary origins still remain mysterious.

Results

A *sex-ratio* Distorter on the X Chromosome (*Dox*)

We previously cloned a *D. simulans* gene, *not much yang* (*nmy*, polytene chromosome position 87F3), in which the homozygous male mutant displays a female-biased sex ratio. This gene belongs to the Winters *sex-ratio* system, one of three independent *sex-ratio* systems found in this species [24]. We inferred that the wild-type (*Nmy*) function is a suppressor of *sex-ratio* distortion, and that there must be a corresponding X-linked *sex-ratio* distorter according to Fisher's principle of sex ratio evolution. By happenstance, we found an X chromosome that did not express the *sex-ratio* phenotype in homozygous *nmy* males (Figure S1). This X chromosome was thought to have a loss-of-function mutation in the gene(s) causing *sex-ratio*. We designate the mutant gene as *distorter on the X* (*dox*). Other X chromosomes, including one from the stock *y* w^{am} v^2 f^{66}, did express *sex-ratio* when tested in the *nmy* background and were postulated to carry the distorting allele *Dox* (Figure S2).

A preliminary mapping of *dox* was carried out through the scheme described in Figure 1. Recombinant X chromosomes were tested for sex ratio (proportion of females or *k*) in the *nmy* background (I in G5 of Figure 1) as well as in the *nmy*/+ background as control (II in G5). A total of 148 X chromosomes tested could be grouped into eight genotypic classes (Figure 2A–2H). Several inferences can be drawn from the results. First, there are two and one recombinants in classes E and F, respectively, which are exceptional and thus informative in the mapping of *dox*, allowing it to be placed closely proximal to *v* at a distance of about 6% (3/51) of the

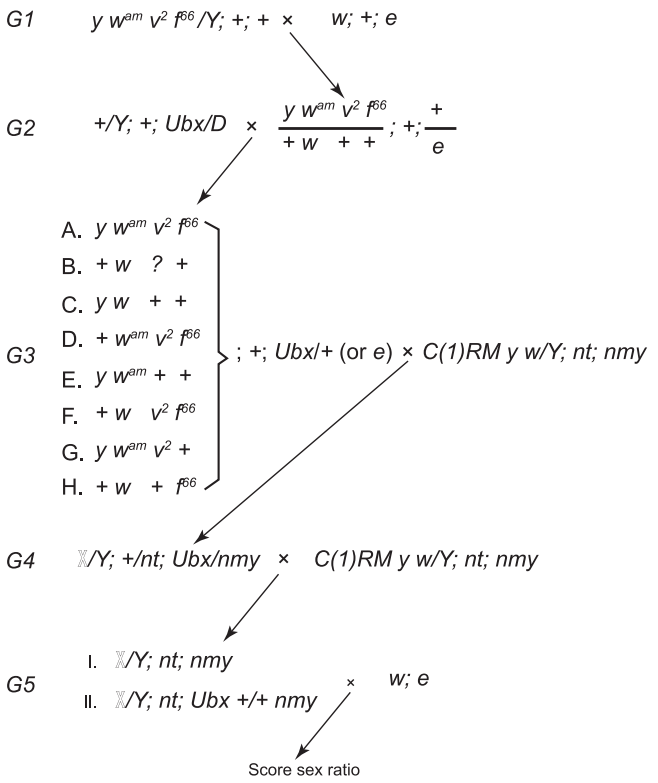

Figure 1. Cross Scheme for Mapping *dox*

One of the parental X chromosomes (*y* w^{am} v^2 f^{66}) has functional distorter(s), whereas the other (*w*) does not. Single-male matings were set up for all X chromosome recombinants in *G3*. All recombinants, represented by X in *G4* and *G5*, were tested for *sex-ratio* in an isogenic background *nt; nmy* in *G5* (I) as well as in a control background of *nt; +/nmy* (II). Two classes of recombinants (F and H) with the same visible phenotype were distinguished by progeny from additional crosses with *y* w^{am} v^2 f^{66} females in *G5*. However, class B (+ *w* ? +) may be a mixture of + *w* + + and + *w* v^2 +, which were not distinguished.
doi:10.1371/journal.pbio.0050293.g001

w–*v* interval. Second, the major *sex-ratio* distorter shows less strength of distortion when a gene in the vicinity of *f* is absent. The reduced distortion can be inferred by comparing classes A ($k \pm$ standard error of the mean [SEM] = 0.803 ± 0.014, $n = 22$), D (0.797 ± 0.019, $n = 7$), and F (0.786 ± 0.020, $n = 22$, excluding one losing the major distorter) with class G that has a significantly lower sex ratio of 0.655 ± 0.013 ($n = 24$) (*t*-test, $p << 0.001$). The first three classes have similar sex ratios (analysis of variance [ANOVA], $p = 0.748$). We call the gene near *f* an *enhancer of Dox* (*E*(*Dox*)) because it alone does not cause sex ratio distortion (class H, 0.509 ± 0.004). In light of the above reasoning, the five class B recombinants showing *sex-ratio* probably have an inferred genotype of *w Dox* v^2 *e(Dox)* (0.686 ± 0.018), the same as class G with respect to *sex-ratio* distorter and enhancer (*t*-test, $p = 0.157$). Finally, based on numerous SNP sites found between the two parental X chromosomes, we genotyped a selected subset of the 148 chromosomes and narrowed the location of *dox* to a region of 215 kb between *CG15316* (8E1–4) and *nej* (8F7–9), which falls within an interval defined by two visible markers *lz* and *v*.

Fine Mapping of *dox*

The fine mapping of *dox* began with the construction of two X chromosomes of lz^s *Dox* v^2 f^{66} and *y* w^{am} *dox*, whose phenotype with regard to *Dox* was confirmed by testing in a

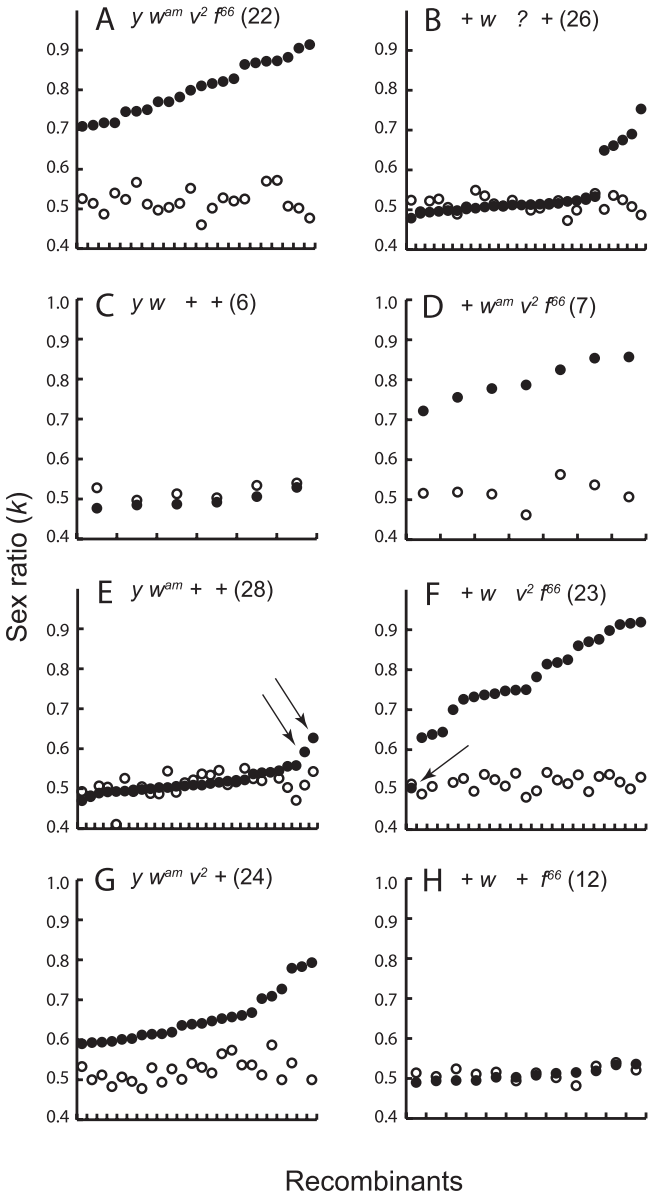

Figure 2. Sex Ratios (*k*) Scored for the Preliminary Mapping

Each recombinant X chromosome in classes A–H (Figure 1) was tested against *nmy* (filled circle) and its sex ratio was rank-ordered within each class. Also shown are the corresponding sex ratios tested against *nmy*/+ (open circles) as control and the number of recombinants tested for each class (in parenthesis). Three exceptional recombinants are indicated with arrows.

doi:10.1371/journal.pbio.0050293.g002

homozygous *nmy* background through the scheme described in Figure 1 (G3 through G5). A cross of $++\ lz^s\ Dox\ v^2\ f^{66}/y\ w^{am}+\ dox\ +\ +$ females to *Ubx*/*D* males was set up, and 324 recombinants with crossovers between *lz* and *v* were obtained. We picked 22 lz^s and 21 $y\ w^{am}\ v^2\ f^{66}$ X chromosomes with crossovers falling between *CG15316* and *nej* to further test their *sex-ratio* phenotype in a homozygous *nmy* background, again using the scheme in Figure 1 (G3 – G5) (Figure 3A). The cross in G4 was carried out at 18 °C so that the *sex-ratio* phenotype of *Dox* can be fully expressed in G5 [24]. Each of the 43 recombinants was unambiguously classified as either *Dox* or *dox*.

Four SNP markers were found in the *CG15316–nej* region (Table S1), and these were used to demarcate the crossover points for the 43 recombinants. There are two *Dox* and five *dox* lines, with their crossovers falling between the markers *5dox_III* and *C14/C17*. We sequenced ~31 kb embracing this region (Figure 3A). The two parental alleles are identical for the 20,791 bp within the *5dox_III–C14/C17* interval, except for a deletion of 105 bp (Δ105) in *dox* (Figure 3B). We confirmed the predicted presence or absence of the Δ105 element in the final seven informative recombinants.

We sequenced six other *D. simulans* strains in the region between the primer pair DoxF4-DoxR4 that spans the Δ105 sequence (Figure 3B; Text S3). Two types of haplotypes were recognized. One is from the *SR6* X chromosome that carries the Paris *sex-ratio* distorters [24,25]. Three copies of a 360-bp repeat were found within this haplotype. The other type is shared by all the other strains, with an insert of 3,833 bp found within the last 360-bp repeat.

This 3,833-bp fragment has sequences homologous to the last three exons from the gene *CG32702* of *D. melanogaster*. The *CG32702* ortholog is missing in the current annotation of *D. simulans* genome (Release 1.0, http://genome.ucsc.edu/). However, we did obtain a sequence of 18.7 kb covering the orthologous *CG32702* region in *D. simulans* as well as its full length cDNA of 11,550 bp (Figure 3B and Text S1). The transcript consists of 15 exons, largely agreeing with the computational annotation of this gene in *D. melanogaster*, except for differences in two splice sites and one extra exon at the 5′ end.

Apparently, this 3,833-bp insert (designated *Tp3833*) was duplicated and transposed from a sequence of 3,549 bp (designated *Tp3549*) in the 3′ region of *CG32702*. Note that one copy of the 360-bp repeat is also present next to *Tp3549*, suggesting that this repeat may have facilitated the transposition. The last two exons and part of exon 13 (Ex13) of *CG32702* are still intact in the *Tp3833* region (*CG32702d*, Figure 3B).

Sequences from the homologous region between DoxF4-DoxR4 were obtained from one strain of each of the sibling species *D. sechellia*, *D. mauritiana*, as well as *D. melanogaster*. All species resemble *SR6* in having various copy numbers of the 360-bp repeat (Figure 3C). A phylogenetic analysis of these 360-bp repeats shows a monophyly of the eight copies from *D. melanogaster*, but a reticulate relationship among the rest, suggesting shared evolutionary history of this intergenic region in the *D. simulans* clade (Figure S3). However, it remains to be determined whether a *Tp3833*-like sequence can be found in *D. mauritiana*. The existence of a functional *Nmy* strongly suggests that a corresponding *sex-ratio* distorter like *Dox* may still segregating in this species [24].

Within *Tp3549*, a fragment of 1,458 bp replaces a fragment of 1,408 bp downstream of the 3′ end of *CG32702* in *D. melanogaster,* and these two sequences have no homology (Figure 3B). Database searches suggest that the 1,458-bp sequence is absent from *D. sechellia*, *D. yakuba*, and *D. erecta*, but some similar fragments of 300–600 bp can be found dispersed in these genomes, often in multiple copies. Transcripts within *Tp3549* were detected, and a new gene, which we designate as *Mother of Dox* (*MDox*), is defined (see below). *Tp3549* and *Tp3833* thus represent a fluid portion of the *Drosophila* genome that occasionally gains new functions.

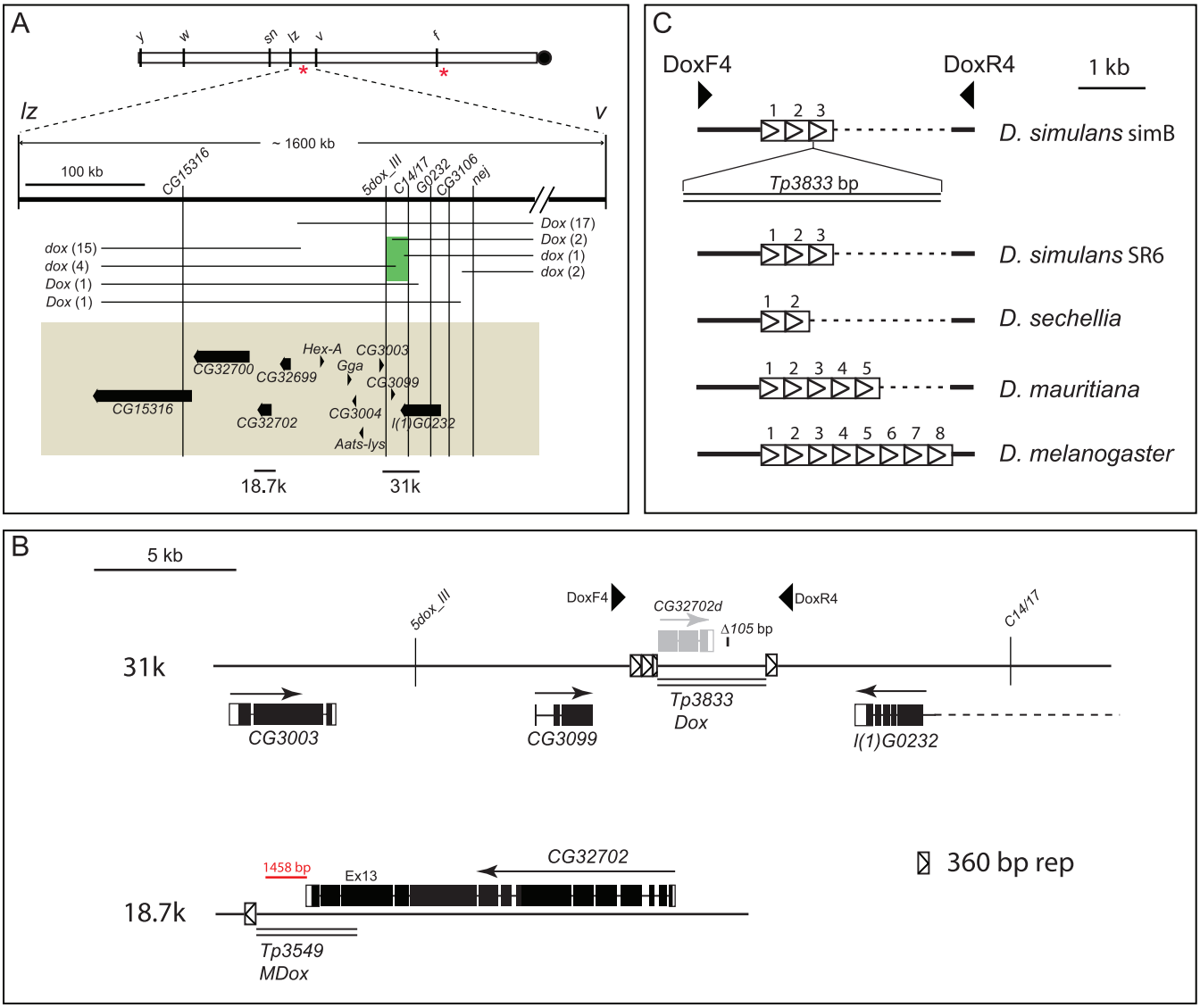

Figure 3. Fine Mapping and Positional Cloning of *dox*

(A) The crossover intervals and the *sex-ratio* phenotype of the definitive 43 recombinants between *lz* and *v*. *dox*: normal sex ratio; *Dox*: sex ratio distorted. The number of similar recombinants is included in parenthesis. The seven most informative recombinant events fall within the interval *5dox_III* and *C14/17* (green region). Some of the annotated genes in *D. melanogaster* in this region are also shown (yellow region) (http://www.flybase.org/cgi-bin/gbrowse/dmel/). The two regions marked as 18.7k and 31k in the *D. simulans* simB strain have been sequenced from PCR products and phage clones. * represents *Dox* at left and *E*(*Dox*) at right.

(B) Annotations of the 18.7k and 31k regions in *D. simulans*. Genes orthologous to *D. melanogster* are shown (arrow: orientation of transcripts; line: introns; open box: untranslated region of mRNA; filled box: coding sequence). A transposition of 3,833 bp (double lines, *Tp3833*) in the *Dox* region can be recognized as originating from the downstream region of *CG32702* (*Tp3549*). The positions of the 105-bp deletion (Δ105) and the exons of *CG32702* within *Tp3833* (*CG32702d* in gray) are shown. A repetitive sequence with a 360-bp consensus has also been recognized in both regions. Primers DoxF4 and DoxR4 were used to amplify this region for cross-species comparisons. In the *Tp3549* region, a sequence of 1,458 bp (red line) has no homolog in *D. melanogaster CG32702*.

(C) Comparison of the *Dox* region among several species of the *D. melanogaster* subgroup. Sequences from eight strains of *D. simulans*, and one strain each from *D. sechellia* (3588), *D. mauritiana* (w12), and *D. melanogaster* (*y; cn bw sp*) were compared. *Tp3833* is present in seven strains of *D. simulans* (represented by simB) but is absent in *SR6*. It is also absent in all other species examined.

doi:10.1371/journal.pbio.0050293.g003

Gene Structure of *Dox*

Initially the truncated version of *CG32702* (*CG32702d*) appeared to be the best candidate for *Dox* because of its perfectly conserved open reading frames (ORFs) and intron–exon boundaries (Figure 3B). However, we have not detected transcripts from *CG32702d*. Extensive 5′- rapid amplification of cDNA ends (RACE) experiments using gene-specific primers targeting *CG32702d* all failed. A 3′-RACE experiment did recover cDNAs, but they could be transcribed from the 3′-end of *CG32702*, not of *CG32702d*. There is a divergent site (C/A) between *Tp3549* and *Tp3833* in the 1,919-bp region corresponding to the last three exons of *CG32702*. Using the primers CG32702seqF26 and CG32702seqR26 (F26 and R26 in Figure 4; Text S3), only the *CG32702* sequence can be

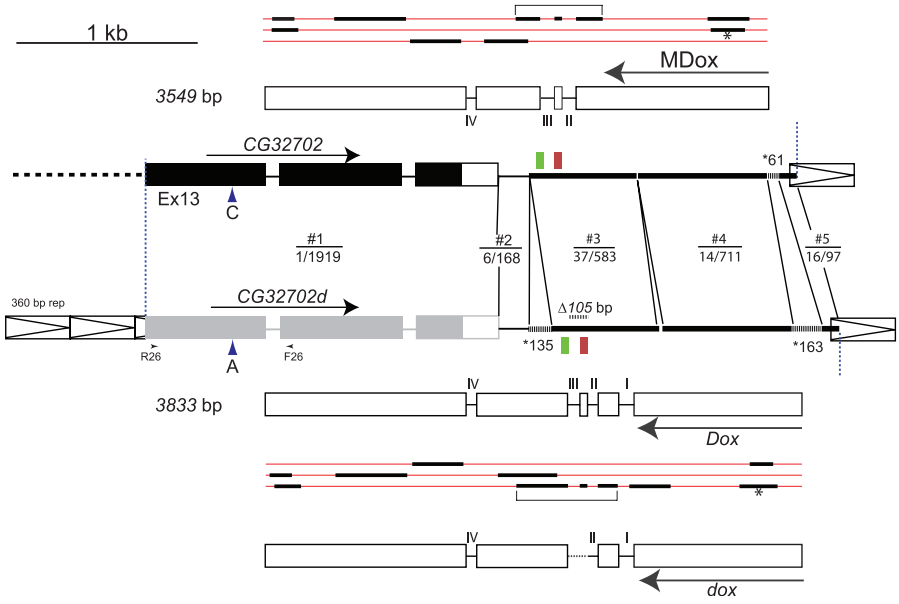

Figure 4. Molecular Structure of *Dox* and *MDox*

Both *Dox* and *MDox* have transcripts in the opposite direction of *CG32702d* or *CG32702*, respectively. The genomic sequences of *Tp3833* (*Dox*) and *Tp3549* (*MDox*) are largely homologous except for one indel of 135 bp (*135) and another short sequence (*61 in *MDox* versus *163 in *Dox*). The 360-bp repetitive sequence may have been involved in the transposition event of *Tp3833*. Five homologous segments of sequences are recognized. The nucleotide divergence is shown for each of them (#1–#5) expressed as nucleotide difference over segment length. Segment #1 corresponds to the last exons of *CG32702* and it has only one nucleotide substitution (A versus C in Ex 13) between these two paralogs. R26 and F26 are the two PCR primers used to amplify genomic DNA and cDNA in this region (see Figure S4). The transcripts of *Dox* and *MDox* were determined by RT-PCR, 5′- and 3′-RACE with primers that can distinguish between these two genes. The intron–exon boundaries of these two genes are largely the same between *Dox* and *Mdox*, so they are annotated together. However, the 91-bp intron I of *Dox* has never been found from *MDox*. Several alternative splicing forms including earlier termination have been found. In some RT-PCR products, introns III and IV of *MDox* are not spliced out. Other splice forms may yet be uncovered. The 105-bp deletion (dashed line) in *dox* causes the loss of exon III in the otherwise identical transcripts as compared to *Dox*. Identical tandem repeats of a 42-bp element (green and red rectangles) are present in both *Dox* and *MDox* transcripts. It is unclear which ORF, if any, is actually translated in each transcript. All potential ORFs larger than 100 bp are shown for all three reading frames (thick black lines on thin red lines). Two ORFs of 157 and 107 aa across the exon III region in the *Dox* and *MDox* transcripts, respectively, are marked with brackets and are the strongest candidate for translation (see Text S2). The best ORF predicted by GENSCAN are marked with an asterisk (http://genes.mit.edu/GENSCAN.html).
doi:10.1371/journal.pbio.0050293.g004

amplified from cDNA (Figure S4). *CG32702d* is therefore unlikely to be transcribed or its expression is too low to be detected by reverse-transcription PCR (RT-PCR).

On the other hand, we have detected transcripts that cover the region of Δ105 in the opposite direction of *CG32702d* (Figure 4). Two transcripts from the allele *Dox* were recovered with either four or three introns. Their full lengths are 2,781 bp and 2,690 bp, respectively. From the allele *dox*, we have also recovered two full-length cDNAs identical to those of *Dox*, except that the exon III, 42 bp in length, is missing because of the deletion Δ105 (Figure 4). This 42-bp element is tandemly repeated in the cDNA of *Dox* but has only one copy in that of *dox*. Within *Tp3549*, we have also recovered a full length cDNA antisense (2,564 bp) to the 3′ end of *CG32702* (Figure 4). *MDox* like *Dox* also has three introns in exactly the same sites, as well as the tandem repeats of 42 bp present in its cDNA (Figure 4).

Surprisingly, all transcripts from the *Dox* and *MDox* loci have very limited coding potential. The largest ORFs of *MDox* in all three frames are shown in Figure 4, and all but one fail to match any known sequences by BLASTX searches through the *nr* database. The one ORF that was predicted by Genscan encodes 62 amino acids (aa), and this ORF highly matches (57/62 or 91% identity) the C terminus of a *D. melanogaster* gene named *CG8664* (located in region 15F7, proximal to the gene *f*). Similarly, only one of the largest ORFs of *Dox* has BLASTX hits. This is again the ORF of 69 aa predicted by Genscan and is homologous to the 62 aa ORF of *MDox*, although only part of it matches to *CG8664* (38/44 or 86% identity) due to a frameshift mutation. *CG8664* has no known biological functions or phenotypes. In the orthologous position of *CG8664* in the current *D. simulans* genome annotation, a fragment of 2,084 bp, instead of a *CG8664* homolog, has been found. Part of this 2,084-bp fragment, approximately equivalent to the 1,458-bp element mentioned above (Figure 3B), is recognized and has a high similarity (99.3% identity) to a region within *Dox*. If the existence of this partial paralog of *Dox* in the *f* region is confirmed by experiment, it would be interesting to test it as the candidate gene for *E(Dox)*.

The pair of tandem 42-bp elements essential for a functional *Dox* are located within an ORF of 157 aa (Figure 4). A 14-aa domain encoded by this 42-bp element has no known functions. If this ORF is ever translated, the tandem 14-aa domains appear to be required for the wild-type function of *Dox* as a *sex-ratio* distorter. Coding or noncoding, the molecular mechanism underlying the effect of *Dox* in rendering Y-bearing sperm dysfunctional awaits further experimental investigation. The wild-type function of *MDox* is not known, although the presence of the critical tandem repeats of the 42-bp element suggests its biochemical similarity to *Dox*.

Nmy Suppresses *Dox* through Homology Effect

The phenotype of *Dox* as a *sex-ratio* distorter is uncovered if its suppressor, *Nmy*, is nonfunctional (Figure 5A) [24]. The *Nmy* transcript appears to form a stem-loop structure with a double-stranded RNA (dsRNA) stem of 345 bp, and small interfering RNAs (siRNAs) produced from the dsRNA stem could target and suppress *Dox* [24]. Hence, homology between *Dox* and *Nmy* is anticipated. Indeed, sequence comparisons suggest that *Nmy* originated from *Dox* through a retrotransposition event [24]. Specifically, the 345-bp dsRNA sequence from *Nmy* has extensive homology to the potential ORF of both *Dox* and *MDox* that contains exon III (Figures 5B). The critical 42-bp element falls within an 85-bp region that has a perfect match with the stem region (positions 264–390 in the alignment of Figure 5C). Whether or how either *Dox* or *MDox* is regulated by these hypothetical siRNAs is currently under investigation.

The possibility that *Dox* evolved solely as a *sex-ratio* distorter and for no other reasons is supported by the normal phenotype of the double mutant *dox; nmy*. We have shown previously that the etiology of the Winters *sex-ratio* is the degeneration of the Y-bearing spermatids during their maturation, as observed both through transmission electron microscopy (TEM) and through light microscopy [24]. We carried out similar observations of the spermatogenesis of *dox; nmy* males at 16 °C. All stages of spermatid maturation appear to be normal as also found in *Dox; Nmy* wild type (Figure 6A–6D, in comparison to Figures 4 and 5 in [24]). Quantitatively, 5.7% ($n = 1108$) of spermatid heads appear to be abnormal under TEM, in a proportion similar to wild-type *Dox*; *Nmy* (5.8%, $n = 1903$). With 4',6-diamidino-2-phenylindole (DAPI) staining, no abnormal spermatid head was observed among the 1,416 heads examined. Consistent with these cytological observations, the sex ratio of progeny from the *dox; nmy* males at 16 °C was 54%. As a comparison, a *dox; Nmy* male was similarly examined. No abnormal heads were observed among 1,058 spermatids, and the sex ratio when tested was also 54%. All the evidence together suggests that *Dox* is not an essential gene and is fully dispensable. *Nmy* is also dispensable if *Dox* is absent.

Evolution of *sex-ratio* in *D. simulans*

The fate of a *sex-ratio* system can be loss, fixation, or stable polymorphism. Apparently, the Winters *sex-ratio* is still segregating in *D. simulans* [24]. The same is true for the Paris *sex-ratio* system that has been found in the same species [21]. Evidence from molecular population genetics shows that the Paris *SR6* X chromosome has swept through African and Indian Ocean islands only recently (less than 20 thousand years ago [ka]) [25]. The presence of a functional *Nmy* suppressor in *D. mauritiana* suggests that the Winters *sex-ratio* evolved in the ancestor of the *D. simulans* clade [24]. The following genetic evidence will enforce the above conclusions and help to compare the evolutionary history of these two *sex-ratio* systems.

We have introgressed the Y chromosome of *D. sechellia* into *D. simulans* (*D. sim Y*[*sech*]) in a background isogenic to simB (Figure S6). The success of this introgression was confirmed by fingerprinting with a Y-specific probe *Y5g* (Figure 7A and Figure S2). The *D. sechellia* Y chromosome was thus tested against the driving effect of either *Dox* (Winters) or *SR6* (Paris). The *Dox*/*Y*[*sech*] male expresses *sex-ratio* if *nmy* is homozygous, but does not if one copy of the functional *Nmy* gene is present (Figure 7B). Hence the *D. sechellia* Y chromosome is equally sensitive to *Dox* as is the *D. simulans* Y chromosome. Intriguingly, *SR6*/*Y*[*sech*] males exhibit male-biased sex ratio distortion ($k = 0.33$). Unfortunately, similar introgression of the Y chromosome from *D. mauritiana* cannot be made because *D. sim Y*[*mau*] is sterile [26].

The above observations are consistent with the earlier estimate that the origin of *Dox* predates speciation among *D. simulans*, *D. mauritiana*, and *D. sechellia* about 200–400 ka [27], whereas *SR6* arose in *D. simulans* after the speciation [24,25]. Assuming that an Y-linked distorter causing male-biased sex ratio distortion has little chance of persistence as compared to an X-linked one causing female-biased sex ratio distortion [13,28], we suppose that the *Y*[*sech*] still bears sensitive sequence to *Dox* as in the ancestral Y of the three species. We suggest that the male-biased sex ratio expressed by *SR6*/*Y*[*sech*] is a sign of evolutionary independence between the *Y*[*sech*] and the *SR6* distorters.

The etiology of *SR6* has been attributed to loss or breakage of the *D. simulans* Y chromosome during meiosis II in *SR6*/*Y*[*sim*] males [29,30]. Our results support earlier findings by showing that male progeny from the *SR6*/*Y*[*sim*] father are sterile at a frequency of 19%. However, the frequency of sterile male progeny from an *SR6*/*Y*[*sech*] father is only 3% (Fisher's exact test, $p < 0.0001$), a number that is not different from the control (2%, Fisher's exact test, $p = 0.284$) (Figure 7C). It is possible that *SR6* does not cause loss or breakage of the *Y*[*sech*], hence the etiology of the male-biased sex ratio may be different from similar *male sex-ratio* (*msr*) cases reported in *D. pseudoobscura* [31] and in *D. affinis* [32], where a large number of nullo XY sperm are produced. The unique cytological mechanism underlying the male-biased sex ratio in *SR6*/*Y*[*sech*] males again suggests that the unequal sex ratio is a neomorph created by a genetic incompatibility between the two chromosomes, rather than a shared evolutionary history of *sex-ratio*.

Discussion

A *sex-ratio* meiotic drive distorter, *Dox*, has been identified. *Dox* is a new gene that arose from yet another new gene *MDox*. Intriguingly, both *MDox* and *Dox* appear to be transcribed as noncoding RNAs or as mRNAs with very limited coding potential. *Dox* was also the precursor for the origin of the autosomal suppressor *Nmy* by a retrotransposition process. *Dox* functions solely as a *sex-ratio* distorter and is not essential, because the mutant *dox* males have normal sex ratio and spermatogenesis. The *Dox*/*Nmy* system is the first that has been characterized at the molecular level for *sex-ratio* meiotic drive, a widespread biological phenomenon that is promoted by the evolution of heteromorphic sex chromosomes.

Nmy Suppresses *Dox*, Possibly through an RNAi Mechanism

The gene structures of *Dox* and *Nmy* strongly suggest that an RNAi mechanism is involved, just as in numerous transgenic studies where inverted repeats (IR) were used to silence target genes in eukaryotes (e.g., [33]). Most likely, the suppression of *Dox* by *Nmy* is through a classic RNAi pathway, also known as post-transcriptional gene silencing (PTGS), which has been under intensive genetic and biochemical studies (reviewed in

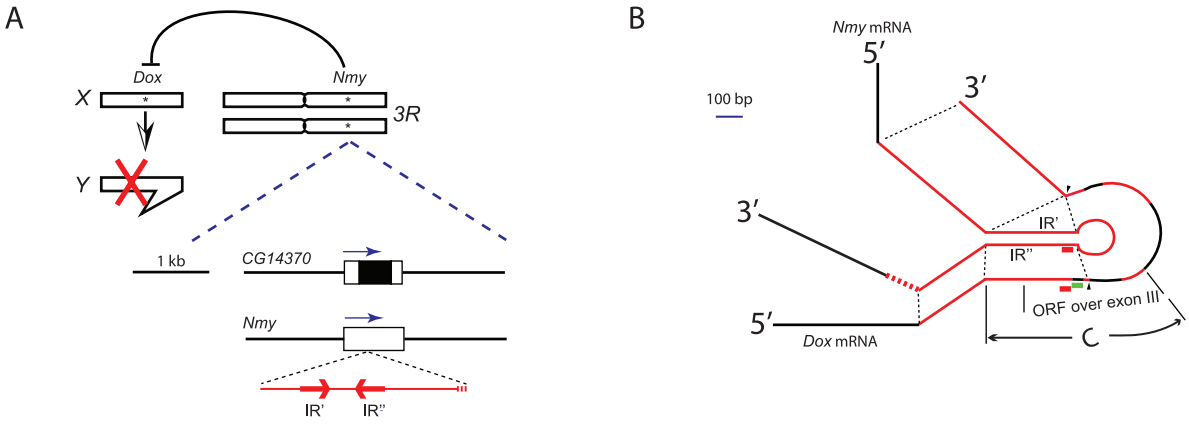

C

```
                844
                |
Dox       1     CATCTAGTTG GCGTGGGGTT TGCCGTACAC GTATACAGCT ATCAATTCGG TTTTTCGAAC CCCATTCGTT ACTTGGGACA GCTGTAAGAA ACATCAATTT
NmyIR'          .......... .......... .......... .......... .G........ .......... .......... .......... .......... .........C ..........
MDox            .......... .......... .......... .......... .G........ .......... .......... .......... .......... .........C ..........
                |
                778
                                                                M  H  S  V  N  P  F  F  Q  Y  V  A  T  F  R  K  E  H  Q  E
Dox       101   GATAAAATAA TCTAAAATAA TCTATCTAAA CAAAAAAAAA ATGCATTCAG TAAATCCGTT TTTCCAATAT GTAGCTACAT TCCGTAAGGA ACATCAAGAA
NmyIR'          .......... .......... ......G.-- -......... ....CC...A ....C..A.. ...T...... .......... .......... .........G
MDox            .......... ....C..C.. .....AG... --....T..T ....C...G. ........C.. ...TG..... .......A.. ......G... G....G...G
                                                                .  P  .  .  .  .  .  E  .  .  .  K  .  .  R  .  .  R  .

                L  K  N  Q  S  V  I  A  Q  R  A  R  D  S  W  N  L  L  T  T  Q  E  K  N  I  Y  R  E  Q  A  R  D  E  Q
Dox       201   CTTAAAAATC AAAGTGTAAT CGCACAAAGA GCTAGGGATT CTTGGAATCT TTTAACTACA CAAGAGAAAA ATATCTACCG CGAACAGGCG CGCGATGAAC
NmyIR'          ........A. .......T.. .......... ..TAGGGA.. .A......G. C......... .......... .......... .......... ..........
MDox            ..A.G.G... ..C.C..T.. ....A..... .....C.... .A...T..TC CC......... ..G....... .......... .......... ..........
                .  R  D  .  R  .  .  .  K  .  .  S  .  .  .  .  Y  S  .  .  .  .  .  .  .  .  .  .  .  .  .  .  .  .  .  .

                  N  R  R  R  R  V  A  V  Q  A  R  D  E  Q  N  R  R  R  R  V  A  V  M  P  A  M  P  C  Q  Q  C  R  Y
Dox       301   AAAATCGGCG TCGGAGAGTG GCAGTACAGG CGCGCGATGA ACAAAATCGG CGTCGGAGAG TGGCAGTAAT GCCAGCGATG CCGTGCCAAC AATGCCGTTA
NmyIR'          .......... .......... ......---- ---------- ---------- ---------- --------.. .......... .......... ..........
MDox            .......... .......... .......... .......... .......... .......... .......... .......... .......... ..........
                  .  .  .  .  .  .  .  .  .  .  .  .  .  .  .  .  .  .  .  .  .  .  .  .  .  .  .  .  .  .  .  .  .  .

                 Y  K  L  A  F  F  A  V  I  S  F  G  F  L  F  L  V  W  K  L  S  S  Y  V  F  P  I  E  N  R  G  K  P
Dox       401   TTACAAATTA GCATTTTTTG CAGTGATATC GTTTGGTTTT CTTTTTTTGG TTTGGAAATT ATCATCCTAT GTATTCCCAA TCGAAAACCG GGGAAAACCG
MDox            .......... ......---- ---------- ---------- ---------- ---------- ---------- ---------- ---------- ----------
                .  .  .  .  .  .

                I  M  A  V  M  P  G  Q  R  C  R  Y  T  K  L  A  F  S  A  L  L  L  F  G  V  V  F  L  V  W  K  L  S  S
Dox       501   ATAATGGCAG TAATGCCGGG CCAACGATGC CGTTATACCA AATTAGCATT TTCTGCACTG CTTTTGTTTG GTGTTGTTTT TTTGGTTTGG AAATTATCAT
MDox            ---------- ---------- ---------- ---------- ---------- -......... .......... .........-- ---------- -----.T----
                                                                        .  .  .  .  .  .  .  .  .  -  .  .  .  -  F  -  -

                  Y  V  F
Dox       601   CCTATGTCTT TTAA
MDox            -----..... ....
                   -  .  .
```

Figure 5. Homology Among *Dox*, *Mdox*, and *Nmy*

(A) Schematic of the Winters *sex-ratio* system. An autosomal suppressor, *Nmy*, is apparently a new gene created by a 2,041-bp insertion (red) in the gene *CG14370*. The insert contains a pair of almost perfect IRs of 345 bp (red arrows, IR′ and IR″) and they are required for the suppression of *Dox*. *Nmy* originated through a retrotransposition event from *Dox*, because all of the 2,041 bp consists of paralogous sequence from cDNA of *Dox* (red line) and the 5′ region upstream of *Dox* transcription (dashed red line) [24].

(B) A detailed comparison between transcripts of *Dox* and *Nmy*. Paralogous sequences are in red. The 5′ and 3′ ends of *Nmy* (black line) are from *CG14370*. IR′ might have duplicated from IR″ after the retroposition [24], while some sequences (black between the two small arrow heads) in *Dox* no longer have paralogs in *Nmy*. The 42-bp elements are shown in red and green color, as in Figure 4. The *dox* allele has lost one of the 42-bp elements in the transcript. A dsRNA stem is presumably formed between the two IR's. The critical region marked as "C" is detailed in (C).

(C) The critical region "C" with a base-by-base comparison among *Dox*, *Nmy*, and *MDox*. Identical bases or amino acids are represented by a period, and deletion by a dash, and divergent bases are in red. This region starts at position 844 (778) of the *Dox* (*MDox*) transcript and the beginning of IR′, respectively. IR′ and IR″ are identical except for a 6-bp (TAGGGA) deletion in IR′ (cyan). The two tandem 42-bp elements are also shown in red and green, respectively on the *Dox* sequence. The amino acids encoded by the ORF in this region are shown in the top (*Dox*) and bottom lines (*MDox*), respectively. These two ORFs have an amino acid identity of 94/107 (88%) and similarity of 100/107 (93%) (underlined).

doi:10.1371/journal.pbio.0050293.g005

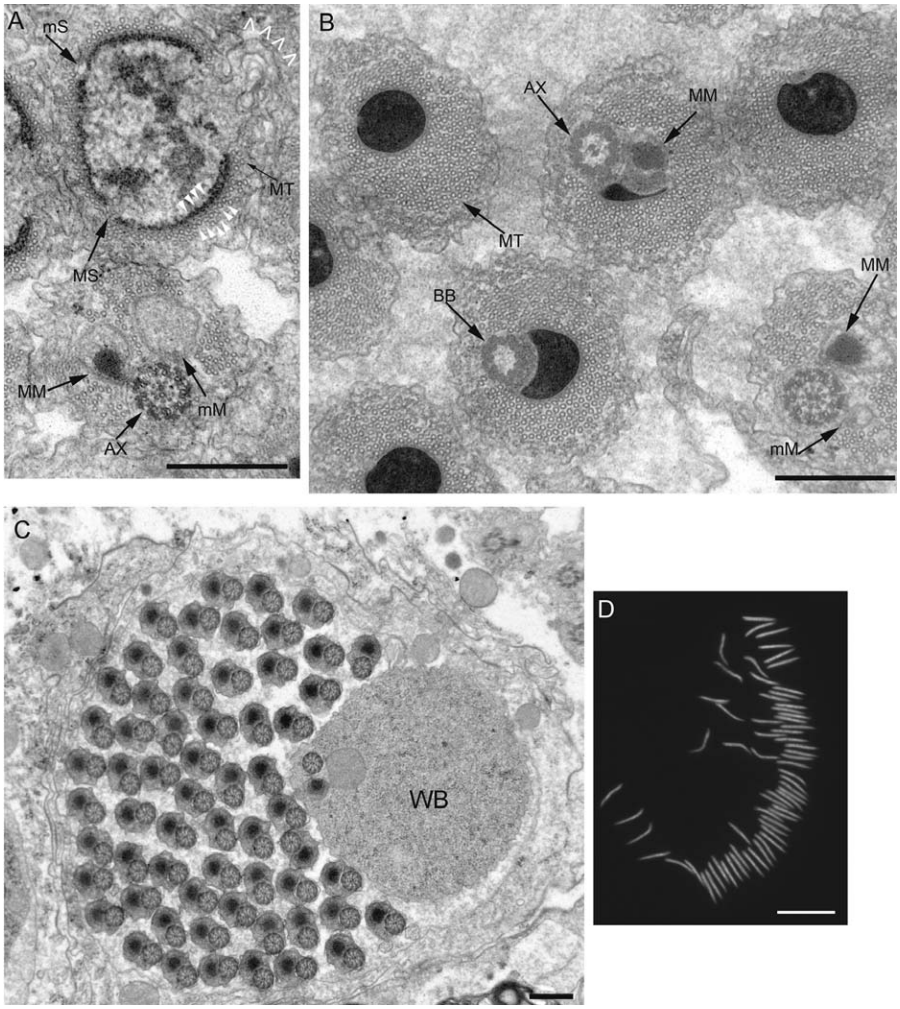

Figure 6. Spermatogenesis of Double-Mutant *dox; nmy* Is Normal

(A–C) TEM images of sperm maturation.

(A) Early post elongation stage of a spermatid head (upper) and tail (lower). Normal nuclear condensation can be seen apposed to rows of microtubules (white arrowheads), while nucleoplasm is eliminated (v).

(B) Late post elongation stage of spermatid heads with homogeneously condensed nuclei (upper left and right). Also note the normal head-tail alignment (middle) and the tail (lower right).

(C) Post individualization stage of a sperm bundle with 61 normal tails and one degenerated tail in the waste bag (WB).

(D) DAPI images of 64 spermatid heads in a bundle at the stage of post elongation.

Abbreviations used in annotation: AX (axoneme); BB (basal body); mM (minor mitochondrial derivative); MM (major mitochondrial derivative); mS (minor strip); MS (major strip); MT (microtubule); WB (waste bag). Scale Bars: 500 nm (A–C); 20 μm (D).

doi:10.1371/journal.pbio.0050293.g006

[34]). In essence, 21–23 nucleotide (nt) siRNAs processed from dsRNA are responsible for guiding the active RNA-induced silencing complex (RISC) to homologous mRNA, resulting in the latter's subsequent cleavage [35]. The PTGS model for *Dox*/*Nmy* interactions can be readily tested by comparing the steady-state mRNA levels of *Dox* between *Dox; Nmy* and *Dox; nmy* males, and by detecting the binding of specific siRNAs with the RISC components. Because PTGS happens in the cytoplasm, and spermatid nuclei within a cyst share the same cytoplamic syncytium, the final gene product of *Dox* likely has a localized deleterious effect in the Y-bearing spermatid nuclei, whereas the presence of a Y or absence of an X must provide the primary cue that eventually leads to abnormal maturation of the Y-bearing sperm heads.

Alternatively, a different type of RNAi mechanism could be involved in the *Dox*/*Nmy* interaction. A class of small RNA in the size range 24–29 nt has been identified as silencing intermediates in the control of repetitive sequences such as retrotransposons [36]. Unlike the classic RNAi machinery, the core proteins do not require DCL-1, DCL-2 and AGO2, and a different type of RNAi pathway (repeat-associated small interfering RNAs or rasiRNAs) has been proposed [36]. The rasiRNA pathway has also been shown to be responsible for silencing a possible cryptic *sex-ratio* meiotic drive distorter, *Ste*, in *D. melanogaster* [37]. The Y-linked *Su*(*Ste*) suppresses the deleterious effects of the X-linked *Ste*, including male sterility and meiotic drive [38]. Both *Ste* and *Su*(*Ste*) consist of repeats that share extensive homology, and rasiRNAs were shown to be the information carrier for the target specificity [36,39,40].

A third possible mechanism for silencing *Dox* might be at transcriptional level in a manner of co-suppression as first observed in plant transgenics, where the expressions of both

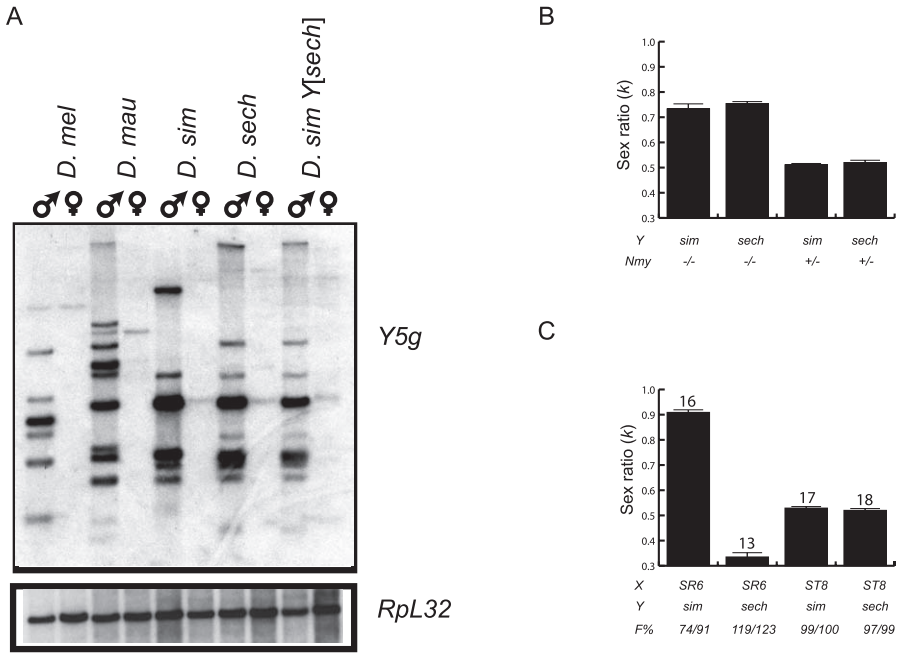

Figure 7. The Y Chromosome from *D. sechellia* Is Sensitive to *Dox* but Distorts *SR6*, Resulting in a Male-Biased Sex Ratio

(A) Fingerprinting the Y chromosomes from *D. melanogaster* sibling species. Genomic DNA was cut with *Hind* III and probed sequentially with the probes *Y5g* and *RpL32*. The probe *Y5g* is composed of sequences from five known Y-specific genes (Figure S6). *RpL32* is an autosomal gene at 99D3. Stocks used: *D. mel*: *D. melanogaster Canton-S*; *D. mau*: *D. mauritiana w12*; *D. sim: D. simulans* simB; *D. sech: D. sechellia 3588*; *D. sim Y*[*sech*]: isogenic to simB (*w; nt; Nmy*) except that the *Y* is from *D. sechellia 3588*, as confirmed here.

(B) Test of the sensitivity of *Y*[*sech*] to *Dox*. *Dox*/*Y*[*sim*] or *Dox*/*Y*[*sech*] males in the background of *nmy* or *nmy*/*Nmy* were constructed by the following scheme: simB or *D. sim Y*[*sech*] males were crossed to *P*40L12 (*w*; *nt*; *P*40L12 *nmy*/*Nmy*] or *P*40B13 (*w*; *nt*; *P*38B13 *Nmy*/*Nmy*) females. Ten sublines of each combination were set up by mating single F1 male (*P*40/*Nmy*) to SR1227 (*w*; *nt*; *nmy*) females. The following four genotypes of males were obtained in the F2: (1) *Dox*/*Y*[*sim*]; *nmy* (*w Dox*/*Y*[*sim*]; *nt*; *P*40L12 *nmy*/*nmy*). (2) *Dox*/*Y*[*sech*]; *nmy* (*w Dox*/*Y*[*sech*]; *nt*; *P*40L12 *nmy*/*nmy*). (3) *Dox*/*Y*[*sim*]; *Nmy*/*nmy* (*w Dox*/*Y*[*sim*]; *nt*; *P*40B13 *Nmy*/*nmy*). (4) *Dox*/*Y*[*sech*]; *Nmy*/*nmy* (*w Dox*/*Y*[*sech*]; *nt*; *P*40B13 *Nmy*/*nmy*). Three males of each subline were tested for *sex-ratio* at room temperature. *Dox; nmy* males express *sex-ratio* regardless of the origin of the Y chromosome. *Y*[*sech*] and *Y*[*sim*] are similar in their sensitivity to the sex ratio distortion effect of *Dox* (*t*-test, $p = 0.341$).

(C) Test the sensitivity of *Y*[*sech*] to *SR6*. The X chromosome *SR6* carries the Paris *sex-ratio* distorters, while *ST8* is the standard nondriving chromosome. Four genotypes of *SR6*/*Y*[*sech*] and its controls were constructed by crossing F1 females obtained from the crosses simB or *D. sim Y*[*sech*] x *C(1)RM yw; nt; Nmy* to *SR6* or *ST8* males: (1) *SR6*/*Y*[*sech*] (*SR6*/*Y*[*sech*], *nt*/+; *Nmy*); (2) *SR6*/*Y*[*sim*] (*SR6*/*Y*[*sim*], *nt*/+; *Nmy*); (3) *ST8*/*Y*[*sech*] (*ST8*/*Y*[*sech*], *nt*/+; *Nmy*); and (4) *ST8*/*Y*[*sim*] (*ST8*/*Y*[*sim*], *nt*/+; *Nmy*). Individual males of the above four genotypes were tested for *sex-ratio* by crossing to three *w; e* females (column ± SEM, with sample size). *SR6* distorts *Y*[*sim*] as reported before [81], and *Nmy* does not suppress *SR6*. Unexpectedly, *Y*[*sech*] actually distorts *SR6*. *F%*: F3 males obtained in the above *sex-ratio* test matings were crossed singly again to three *w; e* females.

doi:10.1371/journal.pbio.0050293.g007

an endogenous gene and the homologous transgene were down-regulated [41]. This type of transcriptional gene silencing (TGS) has been demonstrated in *Drosophila* [42,43], and it requires physical contacts between homologous sequences and Polycomb group (PcG) proteins [44]. Note that an intact pair of inverted repeats is not required for an efficient TGS (e.g.,[44]). In our case, *nmy*[1427] is a loss-of-function mutation that does not have an intact pair of inverted repeats but does have a 1.2-kb sequence paralogous to *Dox*, arguing against this type of TGS as a strong candidate mechanism for silencing *Dox* [24].

Evolutionary Cause for Meiotic Sex Chromosome Inactivation and Achiasmatic Meiosis: The Drive Hypothesis

The X chromosomes of many species are condensed precociously in prophase of meiosis I when active transcription peaks in the autosomes [45]. The existence of meiotic sex chromosome inactivation (MSCI, also known as X chromosome allocycly) has been well established in several model organisms, either directly through the observation of precocious heterochromatin sex bodies [46–48], or indirectly from genetic analysis of X-autosome translocations [49] as well as with genome-wide gene expression studies [50–55]. Recently, MSCI has been demonstrated in *D. melanogaster* by assaying transgenic expressions in the X chromosome [56]. Though sex bodies are the direct evidence for MSCI, they have not been observed in most species examined so far, including *Drosophila* [57]. The status of MSCI may be assayed with more sensitive methods such as the detection of histone modifications that relate to transcriptional activity (e.g., [48]).

There are several hypotheses for the evolution of MSCI. One hypothesis is that MSCI evolves because of a need to suppress recombination between the two sex chromosomes [58]. Another hypothesis was coined as the SAXI hypothesis (sexual antagonism and X inactivation). Because the X spends 2/3 of its evolutionary history in females, the X will be depleted of male-specific genes, and a feminized X would be under selection to be silenced during male meiosis [59]. A third hypothesis has been suggested in the light of the discovery of the meiotic silencing of unpaired DNA (MSUD) in *Neurospora crassa* [60,61]. MSUD is reasoned to have evolved for defending against invasion of transposons [62–64]. The

connection between MSCI and MSUD is supported by the silencing of unpaired chromosomal fragments in the mouse and worm [65,66].

Each of the three hypotheses for MSCI captures only some specific features consequent to the evolution of sex chromosomes, and hence provides only a partial and proximate explanation for the evolution of MSCI. The ultimate cause of MSCI, of course, must be the degeneration of the Y or W chromosome. Following this line of reasoning, we propose yet another hypothesis that we call "the drive hypothesis" for the evolution of MSCI: there is a constant requirement for silencing sex-linked genes including potential *sex-ratio* distorters during meiosis because of an intrinsic conflict over the sex ratio within a genome accompanying sex chromosome evolution.

We believe that the drive hypothesis provides mechanistically superior explanations to the other hypotheses for the evolution of MSCI for the following specific observations: (1) There is a predominant pattern of generating testis-specific genes through retrotransposition between the X chromosomes and autosomes [67–70]. Some of the retrotransposed sequences might be involved in creating new distorters and suppressors. (2) MSCI in the worm and mouse is dependent on a putative RNA-dependent RNA polymerase, suggesting the involvement of an RNAi-like mechanism [71]. The *Dox/Nmy* case provides a strong mechanistic connection between meiotic drive and the evolution of MSCI. Admittedly, it is not an easy task to test empirically and discriminate among the hypotheses described above. Although the drive hypothesis emphasizes the importance of meiotic drive in the evolution of MSCI, other sex-chromosome–specific features such as suppressed recombination, degeneration, and depletion of sex-specific genes could well be different facets of the same evolutionary process. These features may share biochemical components and have reinforced each other over evolutionary time.

In addition to MSCI, achiasmatic meiosis is another evolutionary oddity that might also be rooted in sex chromosome evolution. An achiasmatic meiosis has no crossovers between homologs, even of autosomes. Between 20 and 30 independent evolutionary occurrences of achiasmatic meiosis have been recorded, and all of them are observed in the heterogametic sex [72], with one possible exception in *Tigriopus californicus* [73,74]. Nevertheless, it is reasonable to generalize that achiasmatic meiosis evolves only in the heterogametic sex, as a result of occasional spillover of the molecular machinery that is simultaneously responsible for both suppressing meiotic drive and recombination between the sex chromosomes. This connection between achiasmy and heterogamety was actually presaged by J. B. S. Haldane and J. S. Huxley [75,76], but here we specify meiotic drive as the major evolutionary cause. One would wonder why there are so many *sex-ratio* meiotic drive cases reported in *Drosophila*. Other than the geneticists' proclivity for counting flies in lab, does achiasmatic male meiosis in this genus also contribute to the abundance of meiotic drive systems?

Variations on a Theme: Meiotic Drive in Females

Meiotic drive in ZW females is mechanistically different from that in XY males. For XY males, *sex-ratio* meiotic drive can be achieved either by loss of a sex chromosome during meiosis (meiotic drive sensu stricto) or by abnormal postmeiotic development (gametic drive or meiotic drive sensu lato, as used throughout this article). To prevent gametic drive, stringent control of X-linked genes must be achieved through means such as MSCI. However, in ZW females, only one of the four haploid products will eventually end up in the functional egg during oogenesis and meiotic drive sensu stricto would be an easier means to achieve biased transmission than gametic drive.

For the ZW species, centromere structure and centromere-binding proteins may play an important role in meiotic drive ("centromere drive") [77], and there may be no particular need for evolving MSCI as a defense against gametic drive, although in principle, occasional female gametic drive may still evolve such as a polar body distorter that can kill an egg. Indeed, there is a general lack of cytological observation of MSCI in the ZW females [57,78], with seemingly one proved exception in the caddis fly *Glyphotaelius pelludidus* [79]. Consistent with this observation, there are only two independent origins of ZW achiasmy [72]. Another explanation for the absence of Z allocycly might be due to a lack of selection pressure to evolve *sex-ratio* distorters on the Z chromosome, because male-biased *sex-ratio* distorter cannot persist long in a population [13], therefore it might have left little trace of impact on genomic evolution prior to its disappearance. The question of whether the Z chromosome lacks MSCI deserves special attention because its general absence would be inconsistent with the SAXI or MSUD hypotheses.

Materials and Methods

Fly stocks. The *D. simulans* stocks are: (1) *y* w^{am} v^2 f^{66} from the Tucson *Drosophila* Stock Center; (2) *w; e* and simB (*w; nt; III*) [80]; (3) *C(1)RM y w/*lz^s and *Ubx/D* from J. Coyne; (4) *SSR*12-2-7 (*w*; *nt*; *nmy*) [24]; and (5) Paris *sex-ratio* X chromosome *SR6* and its standard *ST8* as described previously [81]. The *SR6* and *ST8* X chromosomes are maintained by backcrossing males to females of the stock *C(1)RM y w/*lz^s every generation. The *D. sechellia* stock 3588 is from A. Clark [23].

The *D. mauriatiana* × *D. simulans* introgression lines have been described before [18,80]. The following lines were used in this study: heterozygous introgression lines *P*40–46 *nmy*, *P*38–11 *nmy*, *P*38H77 *Nmy*, *P*40L12 *nmy*, and *P*40B13 *Nmy*, all having the genotype *w; nt; P/ III* (*Nmy*) where *P* represents the various semi-dominant *P*-element transgenes *P*[w^+] marking the introgressed *D. mauritiana* material nearby, and *III* (*Nmy*) represents the third chromosome *III* with *Nmy*. These chromosomes are maintained by backcrossing *P/III* males to simB females every generation. The *SSR* (skewed sex ratio) line Q15.3 is from a previous *D. simulans* × *D. sechellia* hybridization experiment [23]. Several stocks were constructed for this study: *C(1)RM y w/w; nt; III* by backcrossing females of *C(1)RM y w/*lz^s to simB males for >19 generations. *C(1)RM y w/w dox*; *nt; nmy* was constructed through a scheme described in Figure S5. Another stock, *w/Y*[*sech*]; *nt; III*, which is isogenic to simB except that the Y chromosome is from *D. sechellia* 3588, was constructed through a scheme described in Figure S6. The stock *y* w^{am} was constructed from the stocks *w; e* and *y* w^{am} v^2 f^{66}. Another stock, *C(1)RM y w /*lz^s v^2 f^{66}, was constructed from *C(1)RM y w/*lz^s and *y* w^{am} v^2 f^{66}.

Fly work. All flies were reared on cornmeal-molasses-agar medium sprinkled with yeast grains at room temperature (22 ± 1 °C) unless otherwise indicated. The sex ratio of a male was scored by mating this male with three tester virgin females, usually of the stock *w; e*, for 7 d before clearing all adults. The progeny were sexed and counted three times until the 19the day. Sex ratio (*k*) was calculated as percentage of females.

Molecular biology. SNPs were discovered by sequencing 500–1,000–bp PCR products from relevant X chromosomes. The primers were designed by targeting the *D. melanogaster* genome (http://www.flybase.org/), and the virtual PCR products were compared to the *D. simulans* sequences (http://genome.wustl.edu/tools/blast) for correcting any mismatches within the primers (Table S1). Genotyping was done

directly by sequencing. Some other key reagents/kits are: LA Taq long PCR kits (Takara); EZ-Tn5 Insertion Kit for sequencing large DNA fragments (Epicentre); Lambda ZAP II vector for genomic library (Stratagene); TRIZOL Reagent for RNA isolation, SuperScript II Reverse Transcriptase and 3′ or 5′–RACE kits (Invitrogen).

Cytology. Light microscopy and TEM procedures have been described previously [24].

Supporting Information

Figure S1. How Was the *sex-ratio* Distorter Discovered?

Q15.3 is one of the original *SSR* (skewed sex ratio) lines reported [23]. This line had been losing the strength of *sex-ratio* distortion by August 2002 ($k = 0.595$; $n = 10$). One male, however, sired an all-female brood (109 F_1). In another test, 150 eggs sired by a single male developed into 126 female adults. All-female broods are very rare for *nmy* stocks. We were curious whether some new *sex-ratio* mutations had been invading the Q15.3 stock. We crossed *P*40–36 males (*w*; *P*[w^+] *nmy*/*Nmy*) en masse to females from the latter all-female brood (A, *G2*). The stock *P*40–36 *nmy* was constructed during the positional cloning of *nmy* [24]. A total of 238 males at *G3* were singly mated to three *w; e* females to score sex ratio, and the genotypes of these males can be readily grouped into 12 phenotypic classes out of 16 possible genotypes (A). Twenty-two males (marked with *) expressed *sex-ratio* ($k \pm \text{SEM} = 0.986 \pm 0.004$, which is significantly stronger than a typical *nmy* male tested at the room temperature with *k* ranging from 0.754 to 0.947). Particularly, nine out of the 22 males sired all-female broods. This observation suggests that the distorter on the X chromosome from Q15.3 is a hypermorph or there are other new enhancers for *sex-ratio*. However, the observed numbers of genotypes 1 and 4, and that of genotypes 9 and 12, are significantly smaller than expected (3/55 versus 27.5/55 from the genotypes 1–4, G-test, $p < 0.001$; 19/59 versus. 29.5/59 from the genotypes 9–12, $p < 0.01$, regardless of the magnitude of the cross-over rate, s, between *e* and *nmy*). One explanation is that the distorter on the X chromosome from *w; e* might have lost its wild-type function. This explanation is supported by a tighter correlation of the *sex-ratio* phenotype with the X chromosome from Q15.3 (w^+) than that from *w; e* (*w*) (19/59 from genotypes 9–12 versus 3/55 from genotypes 1–4, $p = 0.003$). Assuming the crossover rate between *w* and a *sex-ratio* distorter (*D*) is r, and there is a loss-of-function mutation (*d*) from the stock *w; e*, the current observation can be adequately explained as detailed in (B). Note that the genotypes 5–8 and 13–16 in (A) are not informative. From the genotypes 1.1–4.2, r and s can be estimated as 10.98% and 32.53%, respectively. From genotypes 9.1–12.2, these two estimates are 37.33% and 22.79%, respectively. The values of s are consistent with the position of *nmy*, which is roughly in the middle of *Ubx–pe* interval [24], while these two latter mutations are 23.8 cM and 44.9 cM distal from *e*, respectively. *D* could be anywhere on the X proximal to *cv* (1–19.3; 11.1 cM proximal to *w*) [82].

Found at doi:10.1371/journal.pbio.0050293.sg001 (475 KB PDF).

Figure S2. Testing the X Chromosome in the *nmy* Background

This scheme was used to verify that the X from the stock *w; e* has a loss-of-function mutation for the *sex-ratio* distorter. In *G1*, the # symbol represents either *P38–11 nmy* or *P38H77 Nmy* and the X symbol represents the X chromosome from any stocks including the following: *w; nt; III*, *w; e*, and *y* w^{am} v^2 f^{66}. In *G3*, the X chromosomes were tested either in unsuppressing (*nmy*/*nmy*) or suppressing (*nmy*/*Nmy*) background. In *nmy*/*nmy* background, the X chromosomes from *w; nt; III* (simB) and *y* w^{am} v^2 f^{66} expressed strong *sex-ratio*, whereas the X from *w; e* only expressed very weak *sex-ratio* (*t*-test, * $p < 0.05$; *** $p < 0.001$).

Found at doi:10.1371/journal.pbio.0050293.sg002 (233 KB PDF).

Figure S3. Phylogenetic Analysis of the 360-bp Repeats among the *D. melanogaster* Sibling Species

The phylogenetic tree was constructed using MEGA 3.1 with Kimura 2-parameter and Neighbor-Joining algorithm, and was evaluated by bootstrap [83]. These repeats are defined in GenBank accessions EF596890–EF596893, and AE014298.4 (937..1245, 1246..1604, 1605..1963, 1964..2322, 2323..2681, 2682..3040, 3041..3399, 3400..3758). The eight repeats from *D. melanogaster* form a single cluster. However, all the repeats from the other three species are intermingled, suggesting a history of gene conversion and/or incomplete lineage sorting.

Found at doi:10.1371/journal.pbio.0050293.sg003 (215 KB PDF).

Figure S4. No Transcripts from *CG32702d* Were Detected

The primers CG32702seqF26 and CG32702seqR26, which flank both the divergent base and intron 13 (Figure 4), were used to amplify a 774-bp fragment from genomic DNA (gDNA) and a 706-bp from cDNA. The PCR products were cut with *Bsa*WI that has a restriction site at position 463 on the *CG32702* allele but not on the *CG32702d* allele. No cDNA band of 706 bp was detected, suggesting there is no transcription across intron 13 in *CG32702d*. M indicates DNA size marker.

Found at doi:10.1371/journal.pbio.0050293.sg004 (262 KB PDF).

Figure S5. Construction of a Double-Mutant Stock for *dox* and *nmy*, *C(1)RM y w Dox*/*w dox; nt; nmy*

In *G2*, *P*40L12 *nmy* can have recombination with *III* (*Nmy*) to produce P40L12 *Nmy*, which in turn can have recombinations with *nmy* at *G4*. This rare possibility was excluded after *G5* by Southern blots.

Found at doi:10.1371/journal.pbio.0050293.sg005 (224 KB PDF).

Figure S6. Introgression of the Y Chromosome of *D. sechellia* into Pure *D. simulans* Background

(A) The introgression scheme used here is different from previous ones [84,85]. The *D. sechellia* Y chromosome (*Y*[*sech*]) was substituted into a pure *D. simulans* background that is isogenic to simB. *Y*[*sech*] comes from the line 3588 of *D. sechellia*. The symbol # represents possible hybrid chromosome between *D. simulans* and *D. sechellia*. *P*38–11 provides a dominant marker.

(B) A schematic of the Y chromosome (modified from [86]). To verify that the Y introgression line *D. simulans Y*[*sech*] is authentic, we developed a 3.4-kb Y-specific probe (*Y5g*) that was used to fingerprint the Y chromosomes from *D. melanogaster*, *D. simulans*, *D. mauritiana*, and *D. sechellia*. *D. melanogaster* sequences from five Y-specific genes (three from *kl5*, *kl3*, and *kl2*, and two possibly from *ks1* and *ks2*) were used to design PCR primers [87,88]. The five Y-specific PCR products from *D. simulans* are as follows (size in bp): kl5F-kl5R (670), kl2F-kl2R (930), kl3F-kl3R (879), ks1F-ks1R (575), and ks2F-ks2R4 (351). A PCR trick was used to join two DNA fragments as follows: In the first PCR, a chimera primer, which consists of the reverse primer of the first fragment and the antisense forward primer of the second fragment, was used to make an anchored fragment. In the second PCR, the forward primer of the first DNA and the reverse primer of the second DNA were used to amplify a product consisting of these two DNA fragments, with a mix of the anchored fragment and the second DNA as template. *Y5g* was made by joining the above five fragments sequentially, and was confirmed by sequencing. Southern blots using *Y5g* show species-specific pattern for the Y-chromosome (Figure 7A).

Found at doi:10.1371/journal.pbio.0050293.sg006 (304 KB PDF).

Table S1. Primers Used for SNP Markers

Found at doi:10.1371/journal.pbio.0050293.st001 (91 KB DOC).

Text S1. The Gene *CG32702* and Its Transcript in *D. simulans*

Found at doi:10.1371/journal.pbio.0050293.sd001 (35 KB DOC).

Text S2. The Coding Potential of *Dox* and *MDox*

Found at doi:10.1371/journal.pbio.0050293.sd002 (46 KB DOC).

Text S3. Some Primers Used in This Study

Found at doi:10.1371/journal.pbio.0050293.sd003 (26 KB DOC).

Accession Numbers

All sequences have been deposited in the GenBank database (http://www.ncbi.nlm.nih.gov/Genbank/index.html) and have been assigned the accession numbers EF596886-EF596899.

Acknowledgments

We thank Andrew Clark, Catherine Montchamp-Moreau, and the Tucson *Drosophila* Stock Center for stocks; Justin Blumenstiel, Andy Clark, Steve Frank, John Lucchesi, Collin Meiklejohn, Allen Orr, Robert Trivers, Dan Weinreich, and members of the Hartl lab for numerous stimulating discussions related to issues covered in this article; and Marna Costanzo for participating some part of the research. We are grateful to Laurent Keller and two anonymous reviewers whose comments greatly help us to improve the manuscripts. YT is grateful to Louise Trakimas of the Electron Microscopy Facility in Harvard Medical School for her guidance during the TEM

study and William Gelbart and Hans Hofmann for allowing him to use their microscopes.

Author contributions. YT and DLH conceived the research. YT, LA, SBK, YK, and HX performed the experiments. YT analyzed the data. YT and DLH wrote the paper.

Funding. This work was funded by a grant from the National Institutes of Health to DLH and YT (GM65169) and an Emory University Research Council grant to YT.

Competing interests. The authors have declared that no competing interests exist.

References

1. Ohno S (1967) Sex chromosomes and sex-linked genes. Berlin, Heidelberg, New York: Springer-Verlag.
2. Westergaard M (1958) The mechanism of sex determination in dioecious flowering plants. Adv Genet 9: 217–281.
3. Graves JAM (2006) Sex chromosome specialization and degeneration in mammals. Cell 124: 901–914.
4. Liu Z, Moore PH, Ma H, Ackerman CM, Ragiba M, et al. (2004) A primitive Y chromosome in papaya marks the beginning of sex chromosome evolution. Nature 427: 348–352.
5. Peichel CL, Ross JA, Matson CK, Dickson M, Grimwood J, et al. (2004) The master sex-determination locus in three-spine sticklebacks in on a nascent Y chromosome. Curr Biol 14: 1416–1424.
6. Matsuda M, Nagahama Y, Shinomiya A, Sato T, Matsuda C, et al. (2002) *DMY* is a Y-specific DM-domain gene required for male development in the medaka fish. Nature 417: 559–563.
7. Carvalho AB, Clark AG (2005) Y chromosome of *D. pseudoobscura* is not homologous to the ancestral *Drosophila*. Science 307: 108–110.
8. Lahn BT, Page DC (1999) Retroposition of autosomal mRNA yielded testis-specific gene family on human Y chromosome. Nat Genet 21: 429–433.
9. Saxena R, Brown LG, Hawkins T, Alagappan RK, Skaletsky H, et al. (1996) The DAZ gene cluster on the human Y chromosome arose from an autosomal gene that was transposed, repeatedly amplified and pruned. Nat Genet 14: 292–299.
10. Skaletsky H, Kuroda-Kawaguchi T, Minx PJ, Cordum HS, Hillier L, et al. (2003) The male-specific region of the human Y chromosome is a mosaic of discrete sequence classes. Nature 423: 825–837.
11. Lucchesi JC, Kelly WG, Panning B (2005) Chromatin remodeling in dosage compensation. Annu Rev Genet 39: 615–651.
12. Fisher RA (1930) The genetical theory of natural selection. A complete variorium edition. Oxford: Oxford University Press. 318 p.
13. Hamilton WD (1967) Extraordinary sex ratios. Science 156: 477–488.
14. Jaenike J (2001) Sex chromosome meiotic drive. Annu Rev Ecol Syst 32: 25–49.
15. Crow JF (1991) Why is Mendelian segregation so exact? BioEssays 13: 305–312.
16. Hurst LD, Pomiankowski A (1991) Causes of sex ratio bias may account for unisexual sterility in hybrids: a new explanation of Haldane's rule and related phenomena. Genetics 128: 841–858.
17. Frank SA (1991) Divergence of meiotic drive-suppression systems as an explanation for sex-biased hybrid sterility and inviability. Evolution 45: 262–267.
18. Tao Y, Hartl DL (2003) Genetic dissection of hybrid incompatibilities between *Drosophila simulans* and *D. mauritiana*. III. Heterogeneous accumulation of hybrid incompatibilities, degree of dominance, and implications for Haldane's rule. Evolution 57: 2580–2598.
19. Faulhaber SH (1967) An abnormal sex ratio in *Drosophila simulans*. Genetics 56: 189–213.
20. De Magalhães LE, Roveroni IM, Campos SHA (1985) Occurrence of the *sex-ratio* trait in natural populations of *Drosophila simulans* in Brazil. Rev Brasil Genet 8: 449–456.
21. Merçot H, Atlan A, Jacques M, Montchamp-Moreau C (1995) Sex-ratio distortion in *Drosophila simulans*: co-occurence of a meiotic drive and a suppressor of drive. J Evol Biol 8: 283–300.
22. Tao Y, Hartl DL, Laurie CC (2001) Sex-ratio segregation distortion associated with reproductive isolation in *Drosophila*. Proc Natl Acad Sci USA 98: 13183–13188.
23. Dermitzakis ET, Masly JP, Waldrip HM, Clark AG (2000) Non-Mendelian segregation of sex chromosomes in heterospecific Drosophila males. Genetics 154: 687–694.
24. Tao Y, Masly JP, Araripe L, Ke Y, Hartl DL (2007) A *sex-ratio* system in *Drosophila simulans*. I: An autosomal suppressor. PLoS Biol 5: e292. doi:10.1371/journal.pbio.0050292.
25. Derome N, Métayer K, Montchamp-Moreau C, Veuille M (2004) Signature of selective sweep associated with the evolution of *sex-ratio* drive in *Drosophila simulans*. Genetics 166: 1357–1366.
26. Johnson NA, Perez DE, Cabot EL, Hollocher H, Wu C-I (1992) A test of reciprocal X-Y ineractions as a cause of hybrid sterility in *Drosophila*. Nature 358: 751–753.
27. Kliman RM, Andolfatto P, Coyne JA, Depaulis F, Kreitman M, et al. (2000) The population genetics of the origin and divergence of the *Drosophila simulans* complex species. Genetics 156: 1913–1931.
28. Hamilton WD (1979) Wingless and fighting males in fig wasps and other insects. In: Blum MS, Blum NA, editors. Reproductive competition, mate choice and sexual selection in insects. New York and London: Academic Press. pp. 167–220.
29. Montchamp-Moreau C, Joly D (1997) Abnormal spermiogenesis is associated with the X-linked *sex-ratio* trait in *Drosophila simulans*. Heredity 79: 24–30.
30. Cazemajor M, Joly D, Montchamp-Moreau C (2000) *Sex-ratio* drive in *Drosophila simulans* is related to equational non-disjunction of the *Y* chromosome. Genetics 154: 229–236.
31. Cobbs G, Jewell L, Gordon L (1991) Male-sex-ratio trait in *Drosophila pseudoobscura*: Frequency of autosomal aneuploid sperm. Genetics 127: 381–390.
32. Voelker RA (1972) Preliminary characterization of "sex ratio" and rediscovery and reinterpretation of "male sex ratio" in *Drosophila affinis*. Genetics 71: 597–606.
33. Lam G, Thummel CS (2000) Inducible expression of double-stranded RNA directs specific genetic interference in *Drosophila*. Curr Biol 10: 957–963.
34. Tomari Y, Zamore PD (2005) Perspective: machine for RNAi. Genes Dev 19: 517–529.
35. Martinez J, Tuschl T (2004) RISC is a 5' phosphomonoester-producing RNA endonuclease. Genes Dev 18: 975–980.
36. Vagin VV, Sigova A, Li C, Seitz H, Gvozdev V, et al. (2006) A distinct small RNA pathway silences selfish genetic elements in the germline. Science 313: 320–324.
37. Hurst LD (1992) Is *Stellate* a relict meiotic driver? Genetics 130: 229–230.
38. Hardy RW, Lindsley DL, Livak KJ, Lewis B, Siversten AS, et al. (1984) Cytogenetic analysis of a segment of the *Y* chromosome of *Drosophila melanogaster*. Genetics 107: 591–610.
39. Livak KJ (1984) Organization and mapping of a sequence on the *Drosophila melanogaster X* and *Y* chromosomes that is transcribed during spermatogenesis. Genetics 107: 611–634.
40. Aravin AA, Naumova NM, Tulin AV, Vagin VV, Rozovsky YM, et al. (2001) Double-stranded RNA-mediated silencing of genomic tandem repeats and transposable elements in the *D. melanogaster* germline. Curr Biol 11: 1017–1027.
41. Matzke MA, Primig M, Trnovsky J, Matzke AJM (1989) Reversible methylation and inactivation of marker genes in sequentially transformed tobacco plants. EMBO J 8: 643–649.
42. Pal-Bhadra M, Bhadra U, Birchler JA (1997) Cosuppression in Drosophila: Gene silencing of *Alcohol dehydrogenase* by *white-Adh* transgene is *Polycomb* dependent. Cell 90: 479–490.
43. Pal-Bhadra M, Bhadra U, Birchler JA (2002) RNAi related mechanisms affect both transcriptional and posttranscriptional transgene silencing in *Drosophila*. Mol Cell 9: 315–327.
44. Grimaud C, Bantignies F, Pal-Bhadra M, Ghana P, Bhadra U, et al. (2006) RNAi components are required for nuclear clustering of polycomb group response elements. Cell 124: 957–971.
45. Lifschytz E (1972) X-chromosome inactivation: An essential feature of normal spermiogenesis in male heterogauretic organisms. In: Beatty RA, Gluecksohn-Waelsch S, editors. The genetics of the spermatozoon. Edinburgh: University of Edinburgh Press. pp. 223–232.
46. Goldstein P (1982) The synaptonemal complexes of *Caenorhabditis elegans*: pachytene karyotype analysis of male and hemaphrodite wild-type and him mutants. Chromosoma 86: 577–593.
47. Monesi V (1965) Synthetic activities during spermatogenesis in the mouse. Exp Cell Res 39: 197–224.
48. Kelly WG, Schaner CE, Dernburg AF, Lee M-H, Kim SK, et al. (2002) X-chromosome silencing in the germline of *C. elegans*. Development 129: 479–492.
49. Lifschytz E, Lindsley DL (1972) The role of X-chromosome inactivation during spermatogenesis. Proc Natl Acad Sci U S A 69: 182–186.
50. Reinke V, Smith HE, Nance J, Wang J, Van Doren C, et al. (2000) A global profile of germline gene expression in *C. elegans*. Mol Cell 6: 605–616.
51. Parisi M, Nuttall R, Naiman D, Bouffard G, Malley JD, et al. (2003) Paucity of genes on the *Drosophila* X-chromosome showing male-biased expression. Science 299: 697–700.
52. Ranz JM, Castillo-Davis CI, Meiklejohn CD, Hartl DL (2003) Sex-dependent gene expression and evolution of the *Drosophila* transcriptome. Science 300: 1742–1745.
53. Wang PJ, McCarrey JR, Yang F, Page DC (2001) An abundance of X-linked genes expressed in spermatogonia. Nat Genet 27: 422–426.
54. Khil PP, Smirnova NA, Romanienko PJ, Camerini-Otero RD (2004) The mouse X chromosome is enriched for sex-biased genes not subject to selection by meiotic sex chromosome inactivation. Nat Genet 36: 642–646.
55. Kamath RS, Fraser AG, Dong Y, Poulin G, Durbin R, et al. (2003) Systematic functional analysis of the Caenorhabditis elegans genome using RNAi. Nature 421: 231–237.
56. Hense W, Baines JF, Parsch J (2007) X chromosome inactivation during *Drosophila* spermatogenesis. PLoS Biol 5: e273. doi:10.1371/journal.pbio.0050273

57. Solari AJ (1993) Sex chromoosmes and sex determination in vertebrates. Boca Raton: CRC Press, Inc. 308 p.
58. McKee BD, Handel MA (1993) Sex chromosome, recombination, and chromatin conformation. Chromosoma 102: 71–80.
59. Wu C-I, Xu EY (2003) Sexual antagonism and X inactivation - the SAXI hypothesis. Trends Genet 19: 243–247.
60. Shiu PKT, Raju NB, Zickler D, Metzenberg RL (2001) Meiotic silencing by unpaired DNA. Cell 107: 905–916.
61. Lee JT (2005) Sex chromosome inactivation: The importance of pairing. Curr Biol 15: R249–R252.
62. Shiu PKT, Metzenberg RL (2002) Meiotic silencing by unpaired DNA: properties, regulation and suppression. Genetics 161: 1483–1495.
63. Lee DW, Seong K-Y, Pratt RJ, Baker K, Aramayo R (2004) Properties of unpaired DNA required for efficient silencing in *Neurospora crassa*. Genetics 167: 131–150.
64. Lee DW, Pratt RJ, McLaughlin M, Aramayo R (2003) An Argonaute-like protein is required for meiotic silencing. Genetics 164: 821–828.
65. Bean CJ, Schaner CE, Kelly WG (2004) Meiotic pairing and imprinted X chromatin assembly in *Caenorhabditis elegans*. Nat Genet 36: 100–105.
66. Turner JMA, Mahadevaiah SK, Fernandez-Capetillo O, Nussenzweig A, Xu X, et al. (2005) Silencing of unsynapsed meiotic chromosomes in the mouse. Nat Genet 37: 41–47.
67. Emerson JJ, Kaessmann H, Betrán E, Long M (2004) Extensive gene traffic on the mammalian X chromosome. Science 303: 537–540.
68. Betrán E, Thornton K, Long M (2002) Retroposed new genes out the X in *Drosophila*. Genome Res 12: 1854–1859.
69. Warburton PE, Giordano J, Cheung F, Gelfand Y, Benson G (2004) Inverted repeat structure of the human genome: The X-chromosome contains a preponderance of large, highly homologous inverted repeats that contain testes genes. Gen Res 14: 1861–1869.
70. Levine MT, Jones CD, Lindfors HA, Begun DJ (2006) Novel genes dervied from noncoding DNA in *Drosophila melanogaster* are frequently X-linked and exhibit testis-biased expression. Proc Natl Acad Sci U S A 103: 9935–9939.
71. Maine EM, Hauth J, Ratlif T, Vought VE, She X, et al. (2005) EGO-1, a putative RNA-dependent RNA polymerase, is required for heterochromatin assembly on unpaired DNA during *C. elegans* meiosis. Curr Biol 15: 1972–1978.
72. Burt A, Bell G, Harvey PH (1991) Sex differences in recombination. J Evol Biol 4: 259–277.
73. Ar-Rushidi AH (1963) The cytology of achiasmatic meiosis in the female *Tigriopus copepoda*. Chromosoma 13: 526–539.
74. Voordouw MJ, Robinson HE, Anholt BR (2005) Paternal inheritance of the primary sex ratio in a copepod. J Evol Biol 18: 1304–1314.
75. Haldane JBS (1922) Sex ratio and unisexual sterility in hybrid animals. J Genet 12: 101–109.
76. Huxley J (1928) Sexual difference of linkage in *Gammarus chevreuxi*. J Genet 20: 145–156.
77. Malik HS, Henikoff S (2001) Adaptive evolution of Cid, a centromere-specific histone in Drosophila. Genetics 157: 1293–1298.
78. White MJD (1973) Animal cytology and evolution. London: Cambridge University Press.
79. Kiauta B, Lankhorst L (1969) The chromosomes of the caddis-fly, *Glyphotaelius pelludidus* (Retzius, 1783) (Trichopera: Limnephilidae, limnephilinae). Genetica 40: 1–6.
80. Tao Y, Chen S, Hartl DL, Laurie CC (2003) Genetic dissection of hybrid incompatibilities between *Drosophila simulans* and *D. mauritiana*. I. Differential accumulation of hybrid male sterility effects on the *X* and autosomes. Genetics 164: 1383–1397.
81. Montchamp-Moreau C, Ginhoux V, Atlan A (2001) The Y chromosomes of *Drosophila simulans* are highly polymorphic for their ability to suppress *sex-ratio* drive. Evolution 55: 728–737.
82. Barker JSF, Moth JJ (2001) Linkage maps of *D. simulans*: An update of Sturtevant (1929) with additional loci. Dros Inf Serv 84: 205–206.
83. Kumar S, Tamura K, Nei M (2004) MEGA3: Integrated software for molecular evolutionary genetics analysis and sequence alignment. Briefings in Bioinformtics 5: 150–163.
84. Zeng L-W, Singh RS (1993) The genetic basis of Haldane's rule and the nature of asymmetric hybrid male sterility among *Drosophila simulans*, *Drosophila mauritiana* and *Drosophila sechellia*. Genetics 134: 251–260.
85. Johnson NA, Wu C-I (1992) An empirical test of the meiotic drive models of hybrid sterility: sex-ratio data from hybrid between *Drosophila simulans* and *Drosophila sechellia*. Genetics 130: 507–511.
86. Gatti M, Pimpinelli S (1992) Functional elements in *Drosophila melanogaster* heterochromatin. Annu Rev Genet 26: 239–275.
87. Carvalho AB, Lazzaro BP, Clark AG (2000) Y chromosomal fertility factors kl-2 and kl-3 of *Drosophila melanogaster* encode dynein heavy chain polypeptides. Proc Natl Acad Sci U S A 97: 13239–13244.
88. Carvalho AB, Dobo BA, Vibranovski MD, Clark AG (2001) Identification of five new gene son the Y chromosome of *Drosophila melanogaster*. Proc Natl Acad Sci U S A 98: 13225–13230.